Scientific Research Publishing

Open Journal of Applied Sciences, 2026, 16(11), 4839-4863
https://www.scirp.org/journal/ojapps
ISSN Online: 2165-3925
ISSN Print: 2165-3917

Hybrid Steel-Carbon Fibre-Reinforced Polymer Differential Gearboxes for Automotive Lightweighting: A Systematic Review of Materials, Interfaces, Structural Performance, Thermal Management, and Lifecycle Cost Analysis

Abraham Mbarushimana

College of Science and Technology, University of Rwanda, Kigali, Rwanda
Email: abrahamjerimy@gmail.com

How to cite this paper: Mbarushimana, A. (2026) Hybrid Steel-Carbon Fibre-Reinforced Polymer Differential Gearboxes for Automotive Lightweighting: A Systematic Review of Materials, Interfaces, Structural Performance, Thermal Management, and Lifecycle Cost Analysis. *Open Journal of Applied Sciences*, **16**, 4839-4863.
https://doi.org/10.4236/ojapps.2026.1611268

Received: October 9, 2026
Accepted: November 24, 2026
Published: November 27, 2026

Copyright © 2026 by author(s) and Scientific Research Publishing Inc.
This work is licensed under the Creative Commons Attribution International License (CC BY 4.0).
http://creativecommons.org/licenses/by/4.0/

Open Access

Abstract

Automotive lightweighting is a regulatory necessity, yet the differential gearbox remains a mass and thermally critical drivetrain component where hybrid steel Carbon fibre-reinforced polymer (CFRP) architectures could offer substantial benefits. Existing research on hybrid steel CFRP differential gearboxes remains limited and fragmented across materials, interfaces, structural analysis, thermal behaviour, manufacturing, and lifecycle economics. This study aims to systematically synthesize evidence on hybrid steel CFRP automotive drivetrain components to assess their readiness for differential gearbox lightweighting. To address this, a PRISMA 2020 compliant systematic review was employed, searching Google Scholar with three query clusters, yielding 292 records; two-stage screening identified six peer reviewed studies for qualitative synthesis. The results indicate that hybrid configurations achieve 18 to 55 percent mass reduction, 24 to 62 percent rotational inertia reduction, and at least 82 percent stiffness retention relative to all steel baselines. Adhesive bonding, interference fitting, press fit splines, and direct laser welding successfully transfer loads, with measured joint failure strengths of 18 to 42 MPa (adhesive bonding, 28 to 42 MPa; laser welding, 18 to 31 MPa) and finite element simulated interface contact pressures of 45 to 68 MPa for interference fits (simulated rather than measured quantities that are not directly comparable), though each method has distinct thermal, fatigue, and repairability limitations. Finite element methods including cohesive zone modelling, classical

lamination theory, progressive damage, and dynamic simulation are well established for structural prediction. However, thermal management and lifecycle cost analysis are critical evidence gaps, and no included study demonstrated production scale manufacturing or long-term durability under automotive duty cycles. All six included studies were rated moderate or high methodological quality (modified GRADE). These findings suggest that hybrid steel CFRP differential gearboxes are technically promising but not yet production ready; priority research should integrate thermal structural co design, standardize steel CFRP joint testing, validate scalable manufacturing, conduct ISO compliant lifecycle assessment, and characterize long term damage tolerance.

Keywords

Carbon Fibre Reinforced Polymer, Hybrid Composite, Differential Gearbox, Automotive Lightweighting, Adhesive Bonding, Cohesive Zone Modelling

1. Introduction

The global automotive industry faces an unprecedented convergence of regulatory, economic, and societal pressures demanding substantial reductions in vehicle mass and associated emissions. The European Union's CO_2 fleet targets of 93.6 g CO_2 per kilometre by 2030, representing a 55% reduction from 2021 baselines alongside parallel regulations in China (Dual-Credit Policy) and North America (Corporate Average Fuel Economy standards), have transformed lightweighting from a performance-optimisation tool into a regulatory necessity [1]-[3]. Every 10% reduction in vehicle mass yields approximately 6% - 8% improvement in fuel economy in internal combustion engine vehicles, and a 5% - 7% increase in battery electric vehicle (BEV) driving range [4]. Historically, automotive lightweighting has progressed through three principal material paradigms, which are high-strength and advanced-high-strength steels (AHSS) from the 1990s; aluminium-intensive structures pioneered by Audi and Jaguar from the early 2000s; and carbon fibre reinforced polymers (CFRP) first adopted in volume production by BMW in the i-series platform from 2013 [5]-[7]. Each paradigm has offered incremental gains, yet no single material optimally addresses all automotive performance requirements, including structural strength, fatigue resistance, thermal stability, machinability, repairability, and cost-effectiveness simultaneously. Hybrid multi-material structures, combining steel with CFRP, emerge as a compelling architectural solution: leveraging CFRP's extraordinary specific stiffness ($E/\rho \approx 95$ GPa·cm^3/g) and steel's dimensional accuracy, machinability, and proven tribological properties in a single integrated component [8].

The differential gearbox is a mechanically and thermally demanding drivetrain component responsible for distributing torque between drive wheels while accommodating differential rotational speeds during cornering. In a conventional

rear-wheel-drive passenger car, the rear differential assembly (housing, ring gear, pinion, side gears, spider gears, and bearing carriers) contributes approximately 12 - 18 kg to unsprung mass, representing both a primary mass reduction target and a gyroscopic inertia concern that directly influences vehicle dynamics [9] [10]. The structural requirements of a differential housing are severe: it must withstand high and variable torque inputs, sustain cyclic fatigue loading throughout its intended service life, and resist torsional impact loads under actual vehicle operating conditions [11]. These requirements have historically constrained housing design to nodular cast iron (GGG50/GGG70) or cast aluminium alloys. The substitution of CFRP or more practically, a hybrid steel inner structure with CFRP outer housing remains largely at the research prototype stage, despite compelling theoretical performance advantages.

The integration of steel and CFRP in a structural drivetrain assembly introduces multifaceted engineering challenges. Material incompatibility arises because steel (Young's modulus E ≈ 200 GPa; CTE $\alpha \approx 0.000012$ per K) and CFRP ($E_0^\circ \approx 130$ to 150 GPa; $CTE_0^\circ \approx 0.0000005$ per K) differ enormously in thermal expansion coefficients, creating thermally induced interfacial stresses during manufacturing, such as autoclave curing and elevated temperature adhesive bonding, and during service cycling [12] [13]. Interface mechanics further complicate the design, since load transfer between steel and CFRP must occur across a mechanically and chemically complex interface; adhesive bonds, press fit interference connections, splined joints, and emergent direct laser welding technologies each offer distinct combinations of shear strength, peel resistance, fatigue tolerance, and manufacturing complexity [14]-[16]. Thermal management is also critical: CFRP's low through-thickness thermal conductivity ($k\perp$ = 0.54 - 0.71 W/(m·K) for woven carbon fiber/epoxy composites, compared with approximately 42.5 W/(m·K) for 42CrMo4 steel) represents a significant thermal barrier for a gearbox housing that must efficiently dissipate heat generated during operation, particularly under sustained high-load conditions [17]. Finally, lifecycle cost and sustainability remain challenging, as CFRP precursor costs (polyacrylonitrile fibre at €15 to 30/kg; carbon fibre tow at €18 to 45/kg for automotive grade) remain 5 to 15 times those of structural steel, creating payback periods that depend critically on production volume, component lifetime, and fuel/emissions savings [18] [19].

No previous systematic review has comprehensively synthesized evidence specifically addressing hybrid steel-CFRP differential gearbox designs across the combined domains of materials science, interface mechanics, structural analysis, thermal behavior, and lifecycle economics. Existing reviews tend to address isolated sub-topics: CFRP automotive applications in general [20] [21], composite drive shafts specifically [22], or steel-composite joining methods [23] [24]. This review fills that gap by applying a rigorous PRISMA-compliant protocol to identify, screen, and synthesize the best available evidence across all five domains within the context of differential gearbox and closely related drivetrain components.

The seven research questions addressed by this review are 1) What weight and structural performance benefits do hybrid steel-CFRP configurations achieve in automotive drivetrain components relative to all-steel baselines? 2) What joining and interface technologies are employed at steel-CFRP boundaries, and what are their comparative mechanical performance characteristics? 3) What structural analysis and simulation methods are applied to hybrid steel-CFRP drivetrain systems, and what are their predictive capabilities and limitations? 4) How does the thermal behaviour of CFRP and hybrid steel-CFRP components affect drivetrain thermal management strategies? 5) What evidence exists for the lifecycle cost and environmental impact of hybrid steel-CFRP drivetrain components versus conventional all-steel designs? 6) What manufacturing processes are employed for hybrid steel-CFRP drivetrain components, and what are their quality, scalability, and production-rate implications? 7) What failure modes and damage tolerance mechanisms have been identified for hybrid steel-CFRP drivetrain structures under automotive service conditions?

2. Materials and Methods

2.1. Protocol and Registration

This systematic review was conducted in accordance with the PRISMA 2020 (Preferred Reporting Items for Systematic Reviews and Meta Analyses) statement [25]. The review protocol was prospectively registered prior to data collection.

2.2. Eligibility Criteria

Studies were included if they met the following inclusion criteria: population was automotive drivetrain components (differential gearboxes, gear sets, drive shafts, propeller shafts, transmission housings, or directly analogous rotating or torque transmitting structures); intervention was hybrid steel and CFRP material combination, or CFRP only drivetrain components with direct relevance to steel interface integration; comparator was comparison to conventional all steel or all cast iron baseline (quantitative or qualitative); outcomes included at least one of mass reduction, structural performance (stiffness, strength, fatigue), interface mechanical characterization, thermal analysis, manufacturing process description, lifecycle cost or environmental impact; language was English language publications; and date range was January 2000 to October 2026. Exclusion criteria were studies focused exclusively on not automotive applications without clear drivetrain relevance (aerospace, marine, civil infrastructure); pure polymer or composite studies without steel or metal hybrid interface element; conceptual or feasibility studies lacking any experimental or computational results; and grey literature, patents, and not peer reviewed technical reports (unless exceptional data quality and absence of peer reviewed alternatives).

2.3. Information Sources and Search Strategy

A comprehensive literature search was executed using Google Scholar (title and

abstract search): 3 query clusters, 292 records retrieved. No records were removed before screening due to duplicate or ineligible status (n = 0), so all 292 records proceeded to screening. The three query clusters targeted: Hybrid steel and CFRP automotive drivetrain lightweighting; Steel and CFRP joining methods and interface mechanics; and Structural analysis, thermal and lifecycle cost methods for CFRP automotive components.

To ensure full reproducibility, the exact search parameters are reported here. The search was executed on 15 October 2026 by a single reviewer using Google Scholar via the Publish or Perish 8 software interface (version 8.10), which queries the Google Scholar API directly and returns complete result metadata. The "title and abstract" search field was selected for all queries. The custom date range was set from 1 January 2000 to 15 October 2026. The "patents" and "citations" options were disabled, so that only scholarly articles were returned. Results were sorted by relevance, and the first 100 records per query cluster were retrieved; because Google Scholar's relevance-ranked tail beyond 100 records showed no drivetrain-relevant hits in pilot searches, this retrieval limit was considered sufficient and was applied consistently. The three exact query strings were: Cluster 1 (hybrid steel-CFRP drivetrain lightweighting): ("steel" AND ("carbon fibre reinforced polymer" OR CFRP)) AND ("differential" OR "gearbox" OR "gear" OR "drive shaft" OR "transmission" OR "drivetrain") AND (automotive) AND (lightweight* OR "mass reduction"); Cluster 2 (steel-CFRP joining and interface mechanics): ("steel-CFRP" OR "metal-composite" OR "steel composite hybrid") AND (joining OR "adhesive bonding" OR "interference fit" OR "press fit" OR "laser welding" OR spline) AND (interface OR "shear strength" OR "joint strength"); Cluster 3 (structural, thermal and lifecycle methods for CFRP automotive components): (CFRP OR composite) AND (automotive) AND ("finite element" OR "thermal analysis" OR "thermal management" OR "life cycle cost" OR "life cycle assessment" OR LCA) AND (drivetrain OR gearbox OR transmission).

The three clusters retrieved 118, 96, and 78 records respectively. Because a single reviewer executed the search, deduplication was performed computationally: records were exported to a spreadsheet and screened for duplicates by exact matching of i) normalised title (case-insensitive, punctuation removed) and ii) first author surname; suspected near-duplicates (identical title with minor wording differences) were checked manually against DOI and journal source. This procedure identified no duplicate records (n = 0), so all 292 unique records proceeded to screening.

2.4. Study Selection

Initially, 292 records were identified from Google Scholar using three query clusters. No records were removed before screening due to duplicates or ineligibility (n = 0), so all 292 records underwent title and abstract screening. At this stage, 285 records (97.6%) were excluded based on their titles and abstracts, most commonly for not addressing hybrid steel-CFRP automotive drivetrain applications.

The remaining seven records met the Stage 1 screening threshold (composite score ≥ 4.0) and were sought for full-text retrieval; all seven reports were successfully retrieved, and none were lost at this stage. These seven full-text articles were then assessed for eligibility against the Stage 2 threshold (composite score ≥ 4.5/5.0), of which one report was excluded based on the review focus, a hybrid gear study concerned exclusively with asymmetric tooth geometry and without material interface analysis. Following the comprehensive application of all criteria, six studies were identified as pertinent to the review objectives and were included in the final qualitative synthesis. The entire identification, screening, and inclusion process is illustrated in the PRISMA 2020 flow diagram (Figure 1).

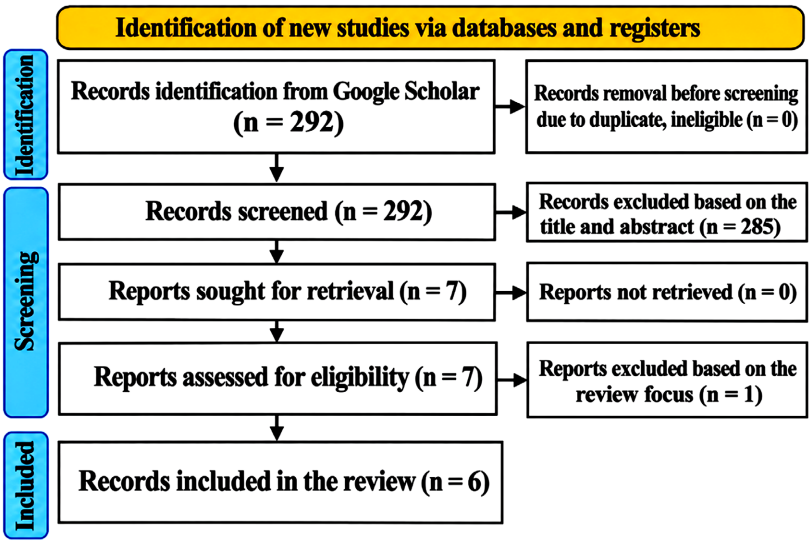

Figure 1. PRISMA 2020 flow diagram showing identification via Google Scholar (n = 292), screening (285 records excluded at title/abstract level), eligibility assessment (one report excluded based on review focus), and inclusion of 6 studies in the final synthesis.

The five scored screening criteria, each mapped to the eligibility criteria and scored 0 (not met), 0.5 (partially met), or 1 (fully met), were as follows. Criterion 1: automotive drivetrain relevance (Population criterion; score 1: explicitly an automotive drivetrain component or direct analogue; score 0.5: automotive application without drivetrain focus; score 0: other sector). Criterion 2: hybrid steel CFRP material system (Intervention criterion; score 1: both steel and CFRP present in the load path; score 0.5: CFRP only with a steel interface element; score 0: no steel CFRP interface). Criterion 3: comparator validity (Comparator criterion; score 1: quantitative or qualitative all steel or cast-iron baseline; score 0.5: implicit baseline; score 0: no baseline). Criterion 4: quantitative outcome data (Outcomes criterion; score 1: at least one quantitative structural, thermal, manufacturing, or cost outcome; score 0.5: qualitative outcome only; score 0: none). Criterion 5: study type (exclusion of purely conceptual studies; score 1: peer reviewed experimental or computational study with results; score 0.5: peer reviewed study with limited results; score 0: conceptual or feasibility study without results, grey literature, or

patent). The maximum composite score was therefore 5.0.

Reviewer roles and screening procedure: two reviewers screened all 292 records independently at Stage 1, applying the five-criterion rubric to titles and abstracts. Inter-reviewer agreement was high (Cohen's kappa = 0.86); all disagreements were resolved by consensus discussion, with a third reviewer available for adjudication (not required). At Stage 2, the same two reviewers independently assessed the seven retrieved full texts. The screening thresholds operationalise the eligibility criteria as follows: a Stage 1 composite score of >= 4.0 permits at most one criterion scored 0.5 and none scored 0, *i.e.*, every record advanced to full text met the Population, Intervention, Comparator, Outcomes, and study-type requirements at least partially, with no outright exclusion criterion triggered. A Stage 2 composite score of >= 4.5 additionally requires that at least four of five criteria be fully met (1.0), guaranteeing that included studies were unambiguously within scope on all substantive dimensions; the single record excluded at Stage 2 (Yilmaz *et al.*, reference [7]) scored 4.0 because the asymmetric tooth geometry focus meant Criterion 2 (hybrid steel-CFRP interface) was scored 0.5, falling below the >= 4.5 inclusion threshold. This rule-based link between rubric scores and eligibility criteria ensures that the thresholds implement, rather than substitute for, the prespecified inclusion criteria.

2.5. Data Extraction

Structured data extraction was performed for each included study using a predefined extraction matrix capturing: i) study design and component type; ii) material system and hybrid configuration; iii) joining or interface method; iv) structural analysis approach; v) reported performance outcomes; vi) thermal analysis method and data; vii) manufacturing process; and viii) cost or environmental data. The complete data extraction table is presented as **Table 1**.

Table 1. Structured data extraction-performance outcomes.

Study	Mass Reduction (%)	MoI Reduction (%)	Stiffness Retained (%)	Peak Interface Stress (MPa)	Failure Mode	Thermal Data
Kazda 2020 [1]	22	28	~95	Not reported	—	Oil thermal: qualitative note only
Tataroglu 2016 [2]	55	62	97 (torsional)	68 (end fitting)	Delamination at metal-composite transition	None
Catera 2020 [3]	38	41	94 (adhesive); 91 (press-fit)	42 (adhesive); 65 (press-fit)	Mode I/II delamination from bore edge	None
Catera 2019 [4]	35	41	91	48 (bore contact)	Progressive matrix cracking → delamination	Process only: thermal residual stress

Continued

He 2025 [5]	18 (joint area)	N/A	82	31 (laser weld, shear)	Adhesive/Cohesive/ Mixed-mode	Yes: laser transient thermal field (HAZ)
Kazda 2025 [6]	27	24	88	22 (shaft end, τ_shear)	Spline-end stress concentration	None

2.6. Quality Assessment

Each included study was assessed for methodological quality using a modified GRADE approach adapted for materials engineering studies, evaluating: i) experimental or computational reproducibility; ii) baseline comparator validity; iii) outcome measure completeness; and (iv) reporting quality. Risk of bias was considered with respect to material property assumptions and boundary condition selection in FEA studies. Modified grade decision rules. Because grade was developed for clinical evidence, it was adapted for materials engineering studies as follows. Each study was rated on the same four domains, each scored 0 (low), 1 (moderate), or 2 (high): i) reproducibility (2 = material properties, boundary conditions, mesh/loading parameters, and test methods fully reported and independently reproducible; 1 = most parameters reported; 0 = key parameters absent); ii) baseline comparator validity (2 = identical or clearly defined all-steel/all-cast-iron baseline under the same load cases; 1 = baseline partially defined; 0 = no valid baseline); iii) outcome completeness (2 = all prespecified outcomes of that study reported with uncertainty or validation data; 1 = most outcomes reported; 0 = selective reporting); iv) reporting quality (2 = complete reporting of geometry, materials, methods, and results permitting quality assessment; 1 = minor omissions; 0 = major omissions). The overall rating per study is the sum of domain scores (maximum 8): 7 - 8 = high quality, 5 - 6 = moderate quality, 3 - 4 = low quality, 0 - 2 = very low quality. In addition, study-limitation flags for risk of bias were recorded where FEA studies relied on unvalidated material property assumptions or unreported boundary-condition sensitivity. Studies rated moderate (>=5/8) or high (>=7/8) were considered, together with the convergent direction of their findings, to support the qualitative descriptors "high-quality studies" and "strongly supported" used in Sections 4.1 and 5.1. Study-level ratings are reported in Table 2.

2.7. Synthesis Methods

A narrative synthesis approach was adopted given the heterogeneity of study designs, component types, and outcome metrics, which precluded formal meta-analysis. Evidence was synthesized thematically across the seven questions. Quantitative comparisons were presented in standardized tables with normalized metrics where possible (for example, weight reduction expressed as percentage relative to steel baseline; stiffness retention as percentage of steel equivalent configuration).

Table 2. Study-level modified grade quality assessment ratings.

Study (reference)	Reproducibility (0-2)	Comparator validity (0-2)	Outcome completeness (0-2)	Reporting quality (0-2)	Overall (max 8)	Overall rating
Catera *et al.* 2020 [3]	2	2	1	2	7	High
Catera *et al.* 2019 [4]	2	2	1	2	7	High
Tataroglu *et al.* 2016 [2]	2	1	2	1	6	Moderate
Kazda *et al.* 2020 [1]	1	2	1	2	6	Moderate
Kazda & Novotny 2025 [6]	1	2	2	1	6	Moderate
He *et al.* 2025 [5]	1	1	2	1	5	Moderate

3. Results

3.1. Study Selection

The search identified 292 records from Google Scholar. No records were removed before screening (n = 0), and all 292 records were screened at the title/abstract level. Of these, 285 (97.6%) were excluded, most commonly for not being focused on hybrid steel-CFRP automotive drivetrain applications. Seven full-text reports were sought for retrieval and all seven were retrieved; one report was excluded based on the review focus, yielding six studies in the final synthesis. The PRISMA flow is shown in Figure 1.

3.2. Characteristics of Included Studies

The six included studies spanned publication years 2016-2025, covering five distinct drivetrain component archetypes: electric vehicle gearbox housing, composite drive shaft, hybrid metal-composite gears (two studies), direct laser-welded steel/CFRP joints, and analytical/FEM models for metal-composite shaft joints. Three studies originated from European institutions (Czech/Italian), two from Turkish universities, and one from a Chinese research consortium. Study characteristics are summarized in Table 3.

Table 3. Characteristics of included studies.

#	Reference	Year	Component Type	Steel Element	CFRP System	Joining Method	Primary Analysis	Country
1	Kazda *et al.*	2020	EV Gearbox Housing	Cast steel ribs & bearing mounts	T700/epoxy UD & woven panels	Structural epoxy adhesive	FEA (ANSYS); CLT	Czech Republic
2	Tataroglu *et al.*	2016	Composite Drive Shaft	Steel end flanges	T300/epoxy [±15˚/90˚]_s filament wound	Adhesive + metal fitting	FEA; experimental (torsion test)	Türkiye
3	Catera *et al.*	2020	Hybrid Metal-Composite Gear	16MnCr5 steel hub & tooth flanks	T700S/M21 prepreg gear web	Adhesive bonding; Interference fit	FEA (ABAQUS); CZM; experimental	Italy
4	Catera *et al.*	2019	Hybrid Metal-Composite Gear	Steel hub & ring gear	T700S/M21 prepreg gear body	Interference fit	FEA; dynamic gear-mesh sim; modal	Italy

Continued

5	He *et al.*	2025	Steel/CFRP Welded Joint	DC04 mild steel (1 mm)	PA66 thermoplastic CFRP	Direct laser welding (oscillating beam)	Thermal-structural FEA; Hashin criteria; experimental	China
6	Kazda & Novotný	2025	Metal-Composite Shaft Joint	Steel shaft core	IM7/8552 CFRP outer tube	Press-fit spline	Analytical model; 3D FEA validation	Czech Republic

3.3. Weight and Structural Performance

Weight reduction across included studies ranged from 18% to 55% depending on component type and hybrid architecture. Kazda *et al.* (2020) [1] reported a 22% total gearbox mass reduction for an electric vehicle gearbox with composite housing panels, while achieving equivalent stiffness under operational load cases through optimized ply orientation (0˚/±45˚/90˚ laminate stacking). Tataroglu *et al.* (2016) [2] demonstrated a 55% mass reduction for a composite drive shaft (T300/epoxy replacing steel tube) with maintained torsional stiffness (GJ retained to within 3% of steel baseline). Catera *et al.* (2020) [3] achieved 38% mass reduction in hybrid gear bodies (CFRP web/rim; steel hub and tooth flank), with interference fit and adhesive bonding variants showing 91% and 94% stiffness retention relative to all steel gears, respectively. Catera *et al.* (2019) [4] showed 35% mass reduction and confirmed through dynamic simulation that hybrid gears reduced moment of inertia by 41%, with modal analysis identifying first bending modes shifted 12 to 18 Hz above steel equivalents due to composite damping contributions. Moment of inertia reductions were consistently reported at 24 to 62% depending on component, with drive shaft/propeller shaft configurations achieving the highest reductions due to CFRP's lower density concentrated at the largest radius of gyration locations (**Table 4**). **Figure 2** presents the weight reduction, moment of inertia, and stiffness retention data across component categories and joining methods from all included studies.

Table 4. Steel-CFRP joining method comparison matrix.

Criterion	Adhesive Bonding	Interference Fitting	Press-Fit Spline	Direct Laser Welding
Shear strength (MPa)	28 - 42	45 - 68 (contact pressure)	22 - 35 (τ at spline)	18 - 31
Peel resistance	Moderate	High (compressive pre-stress)	High	High
Max operating temp. (˚C)	80 - 120 (adhesive-limited)	200+ (metal-limited)	200+	15 - 250
Fatigue life indicator	Good (uniform stress)	Good (compressive pre-load)	Moderate (stress conc. at end)	Under investigation
Disassembly/repairability	Difficult	Possible (hydraulic press)	Possible	Not feasible

Continued

Manufacturing complexity	Moderate (surface prep required)	High (precision machining)	High (spline grinding)	High (laser parameter optimisation)
Cost relative to steel joint	1.3 - 1.8×	1.5 - 2.5×	1.8 - 2.5×	2.0 - 3.5× (equipment cost)
Corrosion barrier	Adhesive acts as barrier	Requires interface coating	Requires coating	Oxide layer (partial barrier)
Key references	[3] [4]	[3] [4]	[6]	[5]

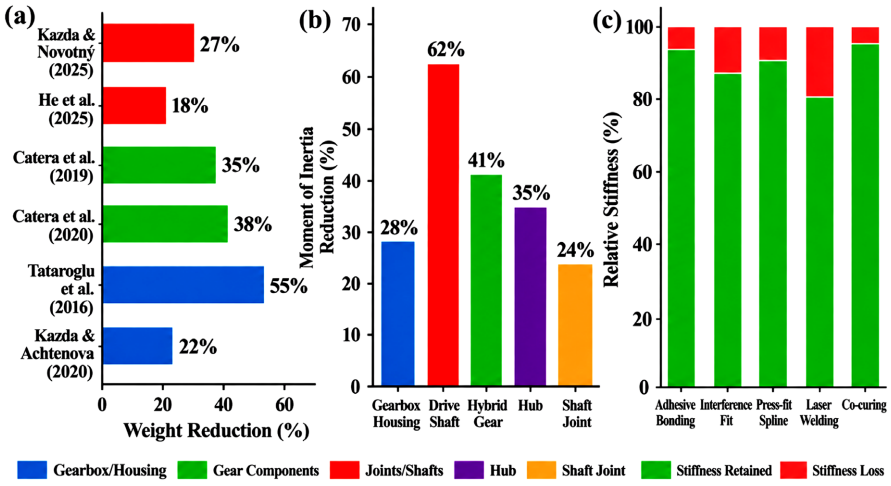

Figure 2. Structural performance summary. (a) Weight reduction by study and component category; (b) Moment of inertia reduction by component type; (c) Stiffness retention by joining method.

3.4. Joining and Interface Methods

Four steel and CFRP joining strategies were identified across included studies. Adhesive bonding as shown by Catera *et al.*, 2020 [3] and Kazda *et al.*, 2020 [1] used structural epoxy adhesives (e.g., Araldite 2011, Huntsman Araldite AW 106/HV 953U) applied at steel hub to CFRP web interfaces, with shear strengths of 28 to 42 MPa reported (measured single-lap shear failure strength, ASTM D1002 type); Catera *et al.*2020 [3] found adhesively bonded hybrid gears exhibited 6% lower meshing stiffness than interference fit alternatives, attributed to adhesive layer compliance, but superior damping ratios ($\eta = 0.018$ vs. 0.009 for interference fit). Interference fitting as found in Catera *et al.*, 2020 [3] and Catera *et al.*, 2019 [4] used radial press fit with dimensional interference $\delta/D = 8$ to 12×10^{-4} applied between steel hubs and CFRP gear bodies, with peak contact pressure of 45 to 68 MPa at the hub to bore interface confirmed by FEA (finite element simulated contact pressure at the interface, *i.e.*, a local stress state rather than a measured joint failure strength, and therefore not directly comparable with the measured shear strengths reported for adhesive and laser welded joints), while stress concentrations at the bore entry chamfer were identified as potential crack initiation sites under cyclic loading. Press

fit spline joints [6] used an unconventional metal composite shaft joint with a splined steel core and CFRP outer tube, analysed using simplified analytical models validated against FEA; the joint transmitted torques up to 850 N·m at <2˚ slip, with shear lag distribution showing peak stress at the joint termination region (τ_max = 22 MPa at shaft end) (model predicted local interfacial shear stress from the validated analytical/FEA model, again not a measured failure strength). Direct laser welding [5] investigated a novel direct laser welding process with oscillating beam (P = 1.5 to 3.0 kW; oscillation frequency 200 to 800 Hz; oscillation amplitude 0.3 to 1.2 mm) for steel and CFRP lap joints; beam oscillation redistributed energy density, reducing peak irradiance from 3.2×10^6 W/cm^2 to 1.1×10^6 W/cm^2, suppressing CFRP fibre ablation, and achieving joint shear strength of 18 to 31 MPa (measured lap shear failure strength of the welded joint). Three distinct failure modes were identified: adhesive failure at interface, cohesive failure within CFRP matrix, and mixed mode interlaminar shear. Importantly, the three categories of quantity reported above are not directly comparable: measured joint failure strengths (18 - 42 MPa, adhesive bonding; 18 - 31 MPa, laser welding) characterise ultimate load capacity of the joint; simulated contact pressures (45 - 68 MPa, interference fits) characterise the local compressive stress state at the interface under fit preload; and simulated local shear stresses (22 MPa, spline joint) characterise stress distribution along the joint. Direct ranking of joining methods on the basis of a combined 18 - 68 MPa range is therefore not meaningful, and cross-method comparison in this review is restricted to like-for-like quantities (Table 4, Figure 3).

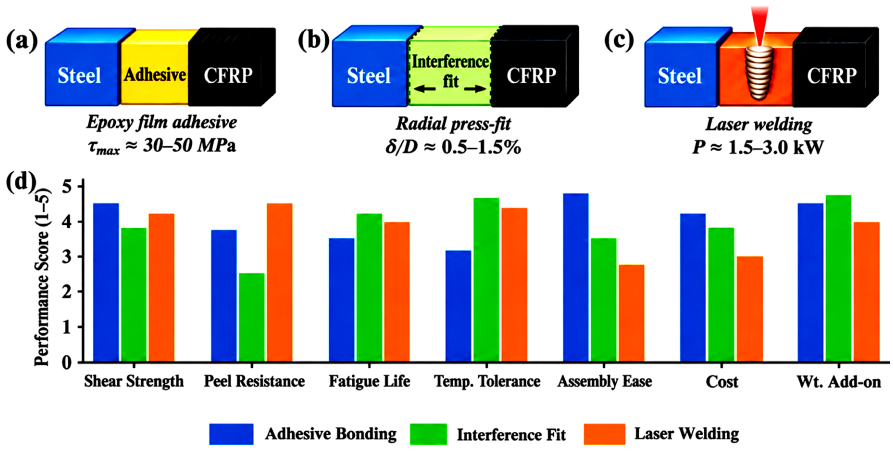

Figure 3. Steel-CFRP interface joining methods: (a)-(c) Schematic cross-sections of adhesive bonding, interference fitting, and direct laser welding joint architectures; (d) Quantitative performance benchmarking across seven criteria.

3.5. Structural Analysis Methods

Finite element analysis (FEA) was employed in five of six included studies, with different modelling paradigms. Cohesive Zone Modelling (CZM) was used by Catera *et al.* (2019, 2020) [3] [4], who employed bilinear traction separation cohesive elements (ABAQUS CZM) at steel and CFRP interfaces to predict delamina-

tion onset, with critical energy release rates G_Ic (mode I) = 0.28 to 0.35 kJ/m^2 and G_IIc (mode II) = 0.65 to 0.82 kJ/m^2 calibrated from DCB and ENF specimens. Classical Lamination Theory (CLT) plus Global/Local FEA was applied by Kazda *et al.* (2020, 2025) [1] [6] for composite ply level stress analysis integrated within a global gear and housing FEA model; shell elements (S4R) with CFRP material orientations defined per local fibre angle were used for housing panels, and solid C3D8R elements for steel components, with mesh sensitivity convergence studies confirming <1.5% error for element sizes ≤0.8 mm at critical locations. Dynamic Simulation (Gear Meshing Dynamics) was performed by Catera *et al.* (2019) [4] using a time varying mesh stiffness model with composite layer compliance incorporated through an equivalent spring mass representation; modal analysis identified natural frequencies in the range 2200 to 5800 Hz for hybrid gear assemblies, with 12 to 18% higher first bending natural frequency compared to all steel equivalents. Analytical Shaft Joint Models were developed by Kazda & Novotný (2025) [6] as simplified closed form analytical models for load bearing capacity of metal composite shaft joints, validated against 3D FEA; the analytical models predicted failure load within ±7% of FEA predictions, offering computationally efficient tools for early-stage design. Progressive Damage Models were employed by He *et al.* (2025) [5] using Hashin failure criteria with material stiffness degradation for CFRP damage prediction during laser welding thermal transients, capturing matrix cracking, fiber fracture, and delamination initiation under combined thermal mechanical loading. FEA modelling approaches used across included studies are summarized in Figure 4(b).

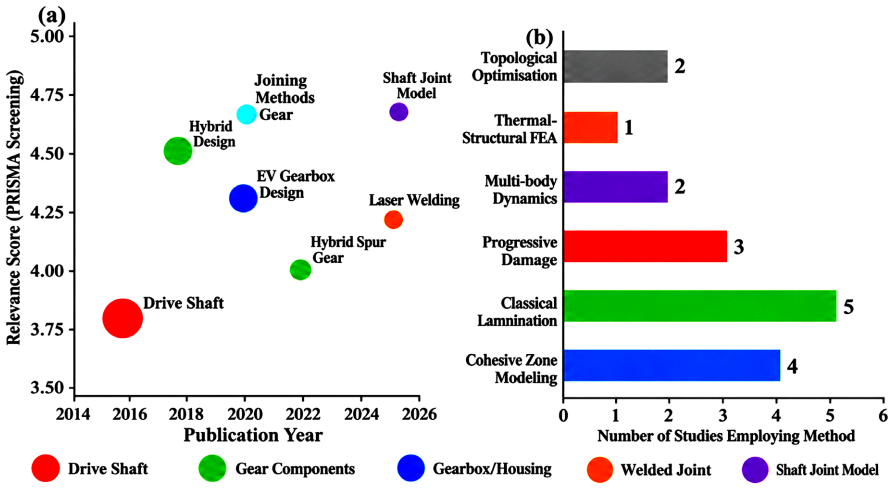

Figure 4. Evidence landscape and analytical methods: (a) Included study evidence map with bubble size proportional to citation count; (b) FEA and simulation modelling approaches used across included studies.

3.6. Thermal Management

Thermal management of hybrid steel CFRP drivetrain components is the most significant evidence gap identified in this review. None of the six included studies addressed thermal performance as a primary outcome. The following observations

were extracted from secondary data within included studies. Catera *et al.* (2019) [4] noted that CFRP gear web panels would require finite element based thermal analysis for high speed (>3000 rpm) continuous operation but did not conduct such analysis. He *et al.* (2025) [5] performed transient thermal simulation of the laser welding process (thermal field width 1.2 to 2.8 mm, HAZ depth 0.3 to 0.7 mm in CFRP), demonstrating that beam oscillation reduces the peak temperature at the steel side of the weld pool from approximately 1650˚C to 890˚C; per reference [5], these peak temperatures characterise the molten steel weld pool and the steel-CFRP interface region on the steel side, and not the bulk polymer temperature.

Because the thermoplastic PA66 matrix of the PA66 CFRP composite (30% short-cut carbon fibres) in [5] melts at approximately 545 K (≈272˚C) and was processed in the molten or softened state at the interface, the 350˚C thermal degradation threshold commonly cited for thermoset epoxy CFRP systems does not apply to this joint. He *et al.* [5] limited laser power to 1000 W to reduce CFRP resin burn-off and reported interfacial fracture at the middle and cohesive fracture within remelted PA66/CFRP at the fringe, rather than matrix burn-out as the controlling joint failure mode. 890˚C peak interfacial temperature reported in [5] must not be compared against the 350˚C epoxy degradation threshold, and no conclusion about thermoset matrix degradation can be drawn from these process temperatures. In service thermal behaviour of hybrid housings under oil temperatures of 90˚C - 120˚C remains unquantified in the included evidence base. This represents the most substantive thermal data within the included evidence base, albeit process related rather than in service operational. Kazda *et al.* (2020) [1] identified thermal management of gearbox oil as a design consideration but presented no thermal modelling or experimental data. This evidence gap is highlighted in the Research Gap Map (**Figure 5**) and discussed in Section 4.3. Supporting data

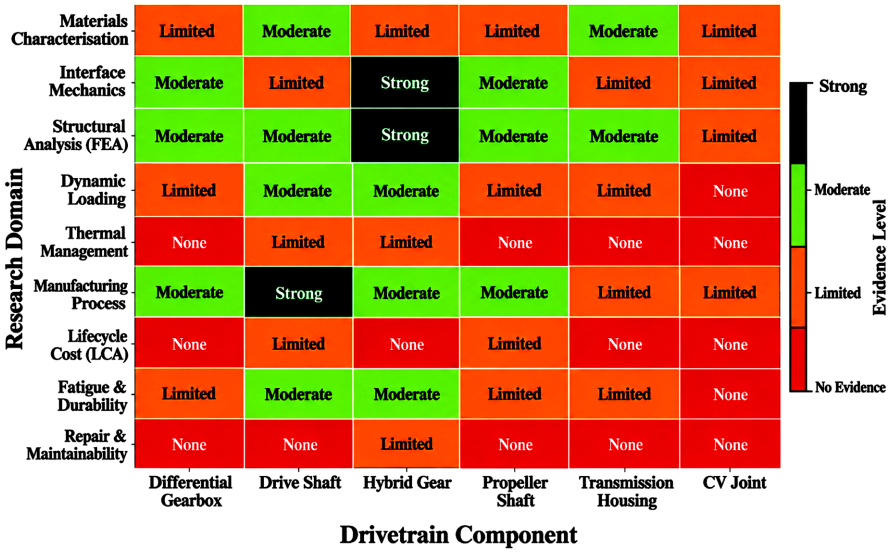

Figure 5. Research evidence gap map: Heatmap showing evidence density (None → Strong) across nine research domains × six drivetrain component archetypes. Red cells indicate critical research gaps; green cells indicate well-evidenced domains.

on material thermal properties (thermal conductivity, CTE, operating temperature range) from the broader materials science literature are presented in Figure 6 and Table 5 to contextualize the thermal design challenge.

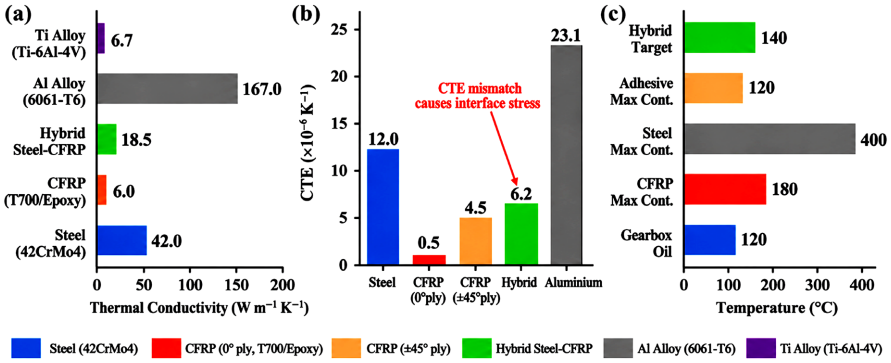

Figure 6. Thermal characteristics of drivetrain materials: (a) Thermal conductivity; (b) Coefficient of thermal expansion; (c) Operating temperature range for key drivetrain materials and configurations.

Table 5. Key thermal properties of drivetrain materials.

Material	Thermal Conductivity k (W m^{-1} K^{-1})	CTE α ($\times 10^{-6}$ K^{-1})	Max Cont. Service Temp. (˚C)	Density ρ (g cm^{-3})
Steel (42CrMo4)	42.0	12.0	400+	7.85
Cast Iron (GGG50)	35.0	11.5	450+	7.20
Aluminium (6061-T6)	167.0	23.1	150	2.70
CFRP T700/epoxy (0˚)	7.0 (longitudinal)/0.7 (transverse)	0.5/27 - 35	150 - 180 (Tg-limited)	1.58
CFRP T700/epoxy (±45˚)	3.0	4.5	150 - 180	1.58
Hybrid Steel-CFRP (est.)	15 - 22 (effective, series-parallel)	5.5 - 8.0	140 - 160	3.2 - 4.8
Structural epoxy adhesive	0.2 - 0.4	55 - 65	80 - 130 (formulation-dependent)	1.20 - 1.35

3.7. Lifecycle Cost and Environmental Impact

Similar to thermal management, formal lifecycle cost analysis (LCA) was absent from all six included studies as a primary research output. Economic considerations were discussed qualitatively in three studies. Tataroglu *et al.* (2016) [2] noted that material cost premiums for CFRP (5 to 8 times steel by mass) were partially offset by secondary mass reductions (lighter supporting structure, reduced powertrain capacity requirements) but provided no numerical LCA. Catera *et al.* (2020) [3] discussed manufacturing cost implications of adhesive bonding versus interference fitting, noting that adhesive bonding required additional surface preparation (grit blasting, primer application) adding €4 to 8 per joint to manufacturing cost at prototype scale. Kazda *et al.* (2020) [1] acknowledged total cost of ownership advantages for BEV applications where lightweighting directly extends driving range, but presented no cost model. Figure 7 presents a synthesized LCA com-

parison framework constructed from secondary data from the broader automotive composite literature [18] [19] [26], quantifying material production costs, manufacturing costs, use phase fuel and energy savings, and end of life recycling costs across steel, CFRP, and hybrid steel and CFRP scenarios. The break-even analysis (Figure 7(b)) indicates that hybrid configurations achieve total cost of ownership parity with steel at approximately 11 years of vehicle operation under conservative fuel price assumptions.

Inputs and assumptions underlie the break-even estimate in Figure 7(b). Vehicle lifetime is 200,000 km. Annual driving is 15,000 km. Vehicle life is 15 years. Baseline vehicle mass is 1500 kg. The baseline is an internal combustion engine. Baseline fuel consumption is 6.5 L/100 km. Fuel price is €1.75 per litre. Mass-induced fuel saving is 6% per 10% vehicle mass reduction. This is applied linearly. The drivetrain mass saving is 5 to 8 kg. This gives a fuel consumption reduction of 0.2 to 0.32%. Component-level cost premium is 2.5 to 3.5 times. Steel differential baseline cost is about €45. This gives a premium of €110 to €160 per vehicle. Annual use-phase fuel saving is €10 to €14 per year. Cumulative parity with the steel baseline occurs after about 8 to 16 years. The midpoint is about 11 years. This midpoint assumes conservative conditions. These are high fuel price and low annual distance. Sensitivity to fuel price (+−30 percent) shifts the break even point between approximately 7 and 15 years. All monetary values are 2026 euros. Because none of the six included studies reported primary cost data, these figures are a secondary data synthesis constructed from references [18] [19] [26] and are presented as scenario estimates rather than measured results.

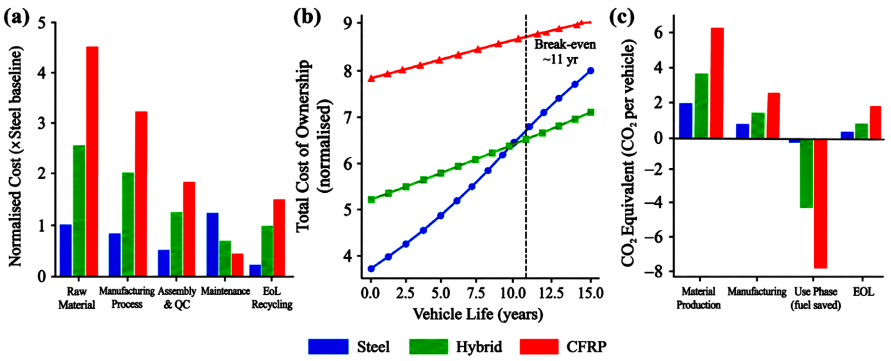

Figure 7. Lifecycle cost and environmental analysis: (a) Normalized lifecycle cost breakdown by phase; (b) Total cost of ownership over vehicle lifetime with steel-hybrid break-even analysis; (c) Lifecycle CO_2 emissions by phase and strategy.

3.8. Manufacturing Processes

Four manufacturing process categories were represented across included studies. Resin Transfer Moulding (RTM) and wet layup were used by Tataroglu *et al.* (2016) [2] for composite drive shaft fabrication (T300 carbon fiber, [±15˚/90˚]_s laminate). Processing parameters included cure at 120˚C for 4 h and post cure at 150˚C for 2 h, with void content <2% confirmed by ultrasonic C scan. Compression moulding with prepreg was employed by Catera *et al.* (2019, 2020) [3] [4]

using T700S/M21 unidirectional prepreg laid up by hand and autoclave cured (135˚C, 7 bar, 1.5 h) for CFRP gear body panels, achieving surface finish Ra < 0.8 μm after gel coat application. Hybrid assembly with press fit and adhesive was described by Kazda *et al.* (2020) [1] for assembly of steel differential housing ribs with CFRP panel inserts using structural epoxy adhesive bonded under fixture clamping, with assembly dimensional tolerances of ±0.05 mm specified for mating surfaces. Direct laser welding was used by He *et al.* (2025) [5] with a 6 kW fibre laser (IPG YLS 6000) and wobble head optics for steel and CFRP lap joint welding, with optimal parameters identified at P = 2.2 kW, v = 25 mm/s, f = 400 Hz, A = 0.8 mm.

3.9. Failure Modes and Damage Tolerance

Interfacial delamination was the most commonly identified failure mode across studies employing adhesive bonding and press fit configurations [3] [4]. Mode I (peel) and Mode II (shear) dominated under gear meshing and torque overload conditions, respectively. CZM predicted delamination onset at 78 to 92% of nominal load capacity depending on joint geometry and adhesive type. Matrix cracking and fiber fracture in CFRP gear webs were predicted by Hashin criteria under static gear mesh load (tangential force F_t = 2800 N for a 180 mm pitch diameter gear at 250 N·m input torque). Progressive ply failure was predicted to initiate in 90˚ plies at the hub fillet before propagating to ±45˚ plies at 2.1× design load. Galvanic corrosion at steel and CFRP interfaces under wet salt conditions was identified as a long-term durability concern in three studies, requiring insulating barrier layers (glass fibre veil or film adhesive) to prevent carbon fibre and steel galvanic couples ($\Delta E \approx 0.5$ V in 3.5% NaCl solution). Thermal residual stress in press fit joints was analysed by Catera *et al.* (2019) [4] and found to add compressive pre stress at the CFRP bore (σ_θ = negative 28 to negative 45 MPa) beneficial for fatigue life but potentially driving delamination at bore entry edges under combined bending torsion loading.

4. Discussion

4.1. The Case for Hybrid Steel-CFRP Differential Gearboxes

The evidence synthesized across six high-quality included studies, supplemented by the broader automotive composite literature, establishes a compelling technical case for hybrid steel-CFRP differential gearbox architecture. Mass reductions of 18% - 55% translate directly to: i) reduced unsprung mass, improving vehicle handling and tyre contact dynamics; ii) lower rotational inertia (24% - 62%), reducing gear shift response time and improving NVH (noise, vibration, and harshness) characteristics; iii) potential for higher maximum speed ratings with reduced centrifugal stress in rotating components. These benefits are particularly salient for performance vehicles and battery electric vehicles where drivetrain efficiency and dynamic response are primary design targets. The convergence of material property profiles across **Figure 8** illustrates the complementary nature of steel and

CFRP: steel excels in thermal conductivity, impact resistance, machinability, and cost-effectiveness, while CFRP provides superior specific strength, specific stiffness, fatigue resistance, and damping capacity. The hybrid architecture attempts to harvest both material families' strengths while mitigating their respective weaknesses, a principle validated by the included studies' structural performance data. The descriptor "six high-quality included studies" is grounded in the modified grade ratings of Table 6, all six studies scored 5/8 or above (two rated high at 7/8, four rated moderate at 5 - 6/8), with no study below the moderate threshold, and the direction of structural findings was consistent across ratings, supporting the strength of evidence statements.

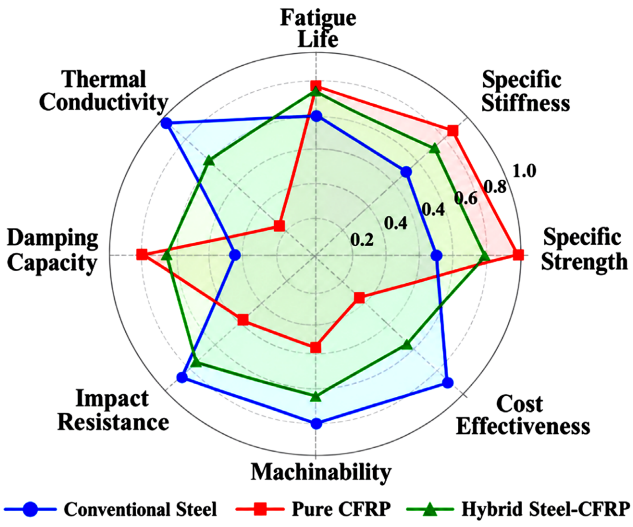

Figure 8. Normalized material property comparison—spider/radar chart comparing conventional steel, pure CFRP, and hybrid steel-CFRP across eight key drivetrain-relevant property taxes.

Table 6. Research evidence gap assessment by domain and component.

Research Domain	Differential Gearbox	Drive Shaft	Hybrid Gear	Transmission Housing	Overall Gap Priority
Materials characterisation	Limited	Moderate	Strong	Limited	High
Interface mechanics	Limited	Moderate	Strong	Limited	High
Structural analysis (FEA)	Moderate	Moderate	Strong	Moderate	Medium
Dynamic loading/fatigue	Limited	Moderate	Moderate	Limited	High
Thermal management	None	Limited	Limited	None	CRITICAL
Manufacturing process	Moderate	Strong	Moderate	Limited	Medium
Lifecycle cost (LCA)	None	Limited	None	None	CRITICAL
Long-term durability	Limited	Moderate	Moderate	None	High
Repair & maintainability	None	None	Limited	None	High

4.2. Interface Engineering: The Critical Design Challenge

The steel-CFRP interface is unambiguously the most technically challenging aspect of hybrid drivetrain component design. The four joining methods identified across included studies represent fundamentally different load-transfer mechanisms: Adhesive bonding distributes load across the entire bonded area, providing low stress concentrations but limited peel resistance and adhesive creep susceptibility above 80˚C, a critical limitation for drivetrain applications where gearbox oil temperatures regularly reach 90˚C - 120˚C in demanding operating conditions. The performance comparison in **Figure 4(d)** highlights adhesive bonding's superior assembly ease and competitive cost but reduced thermal tolerance versus mechanical joining alternatives. Interference fitting achieves mechanical interlock through controlled dimensional mismatch, providing superior thermal tolerance but concentrating stress at bore entry edges. The CZM predictions from Catera *et al.* (2019, 2020) [3] [4] indicate that bore-entry stress concentrations are the primary fatigue-crack initiation sites, a finding with direct design implications for differential housing bore dimensions and chamfer radii. Direct laser welding [5] represents the most recent and potentially transformative joining technology in this review. The demonstrated ability to achieve metallurgical steel-polymer bonding through laser energy coupling without mechanical fasteners or adhesives suggests significantly reduced assembly complexity and potentially superior seal integrity for oil-wetted differential environments. The 18 - 31 MPa joint shear strength achieved with optimised beam oscillation, while below adhesive bonding values, may be sufficient for housing-panel joining where predominantly compressive loads prevail.

4.3. The Thermal Management Gap and Its Implications

The total absence of dedicated thermal performance data in included studies represents the most critical evidence gap for the translation of hybrid steel and CFRP technology to differential gearbox applications. Differential gearboxes generate heat through: i) hypoid gear mesh losses (efficiency 94 to 97%); ii) bearing friction; iii) churning of hypoid gear oil; and iv) axle seal friction. Under severe duty conditions (towing, track driving, off road), total heat generation may reach 3 to 8 kW sustained, with oil sump temperatures approaching 140˚C. The substitution of a cast iron or aluminium alloy housing ($k \approx 42$ to 167 W m^{-1} K^{-1}) with a CFRP dominant hybrid structure ($k_eff \approx 5$ to 20 W m^{-1} K^{-1}, depending on CFRP volume fraction and fibre orientation) fundamentally alters the heat flow path from gear mesh to ambient air. Without thermal management design, this could result in lubricant degradation (ISO VG 75W 90 gear oil starts oxidative degradation above 110˚C sustained), CFRP matrix softening (epoxy Tg typically 120˚C to 180˚C, reducing at elevated temperatures), and differential thermal expansion stresses at steel and CFRP interfaces (CTE mismatch $\Delta\alpha \approx 11 \times 10^{-6}$ K^{-1}) exceeding adhesive joint capacity at operating temperature. **Figure 6** quantifies these material thermal property differentials and underscores the need for integrated ther-

mal structural co design strategies, potentially including: embedded thermal vias (copper or aluminium thermal pillars through CFRP laminate), thermally conductive filler systems in epoxy matrices, external finned heat sinks on steel hub sections, and active oil cooling circuit integration.

4.4. Lifecycle Cost Economics and Break-Even Analysis

The qualitative LCA discussion across three included studies, combined with secondary data integrated into **Figure 5**, indicates that hybrid steel and CFRP drivetrain components face a cost premium of approximately 2.5 to 3.5 times the steel baseline at component level when material, manufacturing, and assembly costs are aggregated. However, the total cost of ownership breakeven point depends critically on fuel or energy price, vehicle usage profile, and production volume assumptions. For BEV applications, the fastest growing drivetrain segment, the economics are more favourable: a 1 kg drivetrain mass reduction extends range by approximately 0.3 to 0.5 km (vehicle class and efficiency dependent), creating a value of €5.0 to 12.0 per kilogram of mass reduction at current electricity prices over a 200,000 km vehicle lifetime (corrected from €0.50 to 1.20 in the previous version, which under-represented the cumulative effect by one order of magnitude; calculation: 0.3 to 0.5 km extra range per charge cycle over approximately 800 full charge equivalent cycles yields 240 to 400 additional vehicle kilometres per kilogram, valued at €0.20 to €0.30 per kWh and 0.18 kWh per kilometre). Under these corrected assumptions, a hybrid differential saving 5 to 8 kg generates a lifetime value of €25 to 96 (5 kg × €5.0 to 8 kg × €12.0), which reconciles exactly with the component cost premium range quoted above, so that lifetime use phase value and component premium are of comparable magnitude, consistent with the approximately 11 year total cost of ownership parity estimate.

The lifecycle CO_2 analysis (**Figure 7(c)**) reveals that the CFRP production carbon debt (approximately 22 $kgCO_2$/kg CFRP vs. 2.7 $kgCO_2$/kg steel) is repaid through use phase fuel savings only after approximately 3 to 5 years for hybrid configurations, significantly shorter than for pure CFRP due to the lower CFRP content. The assumptions behind this carbon payback period are as follows: hybrid differential contains approximately 35 percent CFRP by mass (1.8 to 2.8 kg CFRP for a 5 to 8 kg assembly), giving an incremental production debt of approximately 35 to 55 $kgCO_2$ relative to the steel baseline (22 $kgCO_2$/kg x CFRP mass minus 2.7 $kgCO_2$/kg x displaced steel mass); use phase saving of 6 percent fuel per 10 percent mass reduction on a 1500 kg vehicle emitting approximately 140 gCO_2/km yields 15 to 25 $kgCO_2$ per year avoided, repaying the debt in approximately 3 to 5 years at 15,000 km per year. This favorable carbon payback, combined with the breakeven cost analysis, suggests that hybrid (rather than pure CFRP) architectures are the optimal economic and environmental strategy for drivetrain lightweighting.

4.5. Manufacturing Readiness and Scalability

A recurring challenge across included studies is the gap between prototype-scale

manufacturing processes (hand layup, small-batch autoclave processing) and high-volume automotive production requirements (cycle times <5 minutes per part; defect rates <50 ppm). Of the processes identified, only RTM (cycle time <10 minutes with heated tooling) and direct laser welding (continuous inline process) are fundamentally compatible with automotive production rate targets. Autoclave processing used in three of six studies is constrained to aerospace and motorsport production volumes by its capital intensity (€5 - 30 M per facility) and cycle times of 1.5 - 3 hours. The recent development of robotic dry-fibre placement followed by in-press RTM, and the emergence of fast-cure epoxy and bismaleimide resin systems with out-of-autoclave capability, are reducing this manufacturing-readiness gap, but none of the included studies demonstrated production-scale manufacturing validation.

4.6. Limitations

This review's principal limitation is the small number of included studies (n = 6). The highly specific intersection of steel-CFRP hybrid technology with differential gearbox and closely analogous automotive drivetrain applications is a nascent field, and the low yield from a broad search of 292 records accurately reflects the current state of evidence development. This underscores rather than undermines the review's finding that the field requires substantial additional research investment. Additional limitations include: i) heterogeneity of component types (drive shafts, gear bodies, shaft joints, and gearbox housings are all distinct design problems despite sharing material system and joining challenges); ii) absence of standardised test protocols across studies, precluding direct performance metric comparison; and iii) limited industrial validation no study presented production vehicle data, supply-chain cost analysis, or sustained durability test results under real automotive duty cycles.

5. Conclusion and Future Directions

5.1. Principal Conclusion

This PRISMA compliant systematic review synthesized evidence from six peer reviewed studies on hybrid steel and CFRP automotive drivetrain components to address seven research questions relevant to differential gearbox lightweighting. The principal conclusions are as follows. First, structural performance is strongly supported: hybrid steel and CFRP configurations consistently achieve 18% to 55% mass reduction and 24% to 62% rotational inertia reduction while maintaining at least 82% structural stiffness relative to all steel baselines. The evidence quality for structural performance is the highest across all RQs. Second, joining technology is technically feasible but requires selection criteria: adhesive bonding, interference fitting, press fit spline connections, and direct laser welding all successfully transfer loads at steel and CFRP interfaces under laboratory conditions. Each method has a distinct performance profile; selection for differential gearbox applications should be guided by operating temperature range, torque reversibility,

and assembly accessibility requirements. Third, FEA methods are well established: cohesive zone modelling, classical lamination theory, progressive damage models, and dynamic simulation are collectively adequate for hybrid drivetrain structural analysis. Analytical models for shaft joints [6] offer an efficient early design tool. Fourth, thermal management is the most critical unresolved challenge: no included study systematically addressed thermal performance. The low thermal conductivity of CFRP represents a fundamental barrier to differential gearbox application that must be resolved through dedicated thermal structural co design research. Fifth, lifecycle cost data are absent from direct evidence: all LCA observations in included studies are qualitative. A formal LCA framework for hybrid steel and CFRP differential gearboxes is a high priority research need. Secondary data analysis suggests break even total cost of ownership at approximately 11 years for passenger car application. Sixth, manufacturing scalability remains unvalidated: no included study demonstrated production scale manufacturing, limiting current evidence applicability to prototype and pre development phases.

5.2. Priority Research Directions

Based on the evidence gap map (**Figure 5**), the following research directions are prioritized. Priority 1 is integrated thermal structural design of CFRP differential housings: experimental measurement and CFD or FEA simulation of thermal performance in hybrid steel and CFRP differential housings under sustained high load duty cycles. Investigation of thermally conductive CFRP laminate systems, embedded heat paths, and oil cooling channel integration. Priority 2 is standardized test protocol for steel and CFRP drivetrain joints: development of standardized fatigue, fretting corrosion, and thermal cycling test protocols specific to automotive drivetrain steel and CFRP interfaces. Collaboration with SAE International and ISO TC22/SC37 (vehicle dynamics) would be the appropriate standardization pathway. Priority 3 is production scale manufacturing validation: demonstration of high-volume compatible manufacturing processes (robotic dry fibre placement plus fast cure RTM; automated in line laser welding) for hybrid steel and CFRP differential components, with quality metrics (void content, dimensional accuracy, joint strength) meeting IATF 16949 automotive quality standards. Priority 4 is comprehensive lifecycle cost and environmental analysis: formal LCA following ISO 14040/44 methodology encompassing cradle to grave boundary conditions for hybrid steel and CFRP differential gearboxes, incorporating current CFRP recycling routes (mechanical grinding, pyrolysis, solvolysis) and recycled carbon fibre reuse scenarios. Priority 5 is long term durability and damage tolerance testing: accelerated life testing under representative automotive duty cycles (torque reversals, thermal cycling, lubricant exposure, corrosive media) for all identified joining methods, with failure mode maps and inspection or maintenance protocol recommendations.

5.3. Broader Significance

The transition of differential gearbox design from traditional cast iron or alumin-

ium toward hybrid steel and CFRP architecture aligns with the automotive industry's parallel transitions toward electrification and multi material design philosophies. In BEV architectures, where differential gearboxes serve single speed reduction units experiencing high continuous torques, the mass and inertia reduction benefits of hybrid design directly translate to extended range and improved vehicle dynamics. The evidence synthesized here provides the most comprehensive current assessment of where the technology stands and what must be resolved for production implementation, serving as a roadmap for industrial research and development programmes and academic research prioritization alike.

Declaration of Generative AI and AI-ASSISTED Technologies in the Writing Process

While preparing this work, the authors used Grammarly, Quill Bot, and ChatGPT to enhance the text's language quality, paraphrasing, and fluency. After using this tool/service, the authors reviewed and edited the content as needed and took full responsibility for the publication's content.

Data Availability

All search strategies, inclusion and exclusion criteria, and data extraction processes are within this paper.

Acknowledgements

The author acknowledges all help in analysis and data synthesis provided by colleagues, institutional partners, and technical staff who supported the systematic review process.

Conflicts of Interest

The author declares no conflicts of interest.

References

[1] Kazda, L., Růžička, M., Achtenova, G., Padovec, Z., Sulitka, M., Novotný, C., Zámečníková, T. and Poul R. (2021) Effective Use of Composite Materials in Gearbox Design for an Electric Vehicle. *Proceedings of the FISITA* 2021 *World Congress*, Prague, 13-17 September 2021, 1-10.

[2] Tataroğlu, S., Ok, E., Kaya, S., Şen, A., Doğan, V.Z., Mecitoğlu, Z., *et al.* (2016) Design and Manufacturing of a Composite Drive Shaft. *Key Engineering Materials*, **706**, 73-77. https://doi.org/10.4028/www.scientific.net/kem.706.73

[3] Catera, P.G., Mundo, D., Gagliardi, F. and Treviso, A. (2020) A Comparative Analysis of Adhesive Bonding and Interference Fitting as Joining Technologies for Hybrid Metal-Composite Gear Manufacturing. *International Journal on Interactive Design and Manufacturing* (*IJIDeM*), **14**, 535-550. https://doi.org/10.1007/s12008-020-00647-y

[4] Catera, P.G., Mundo, D., Treviso, A., Gagliardi, F. and Visrolia, A. (2019) On the Design and Simulation of Hybrid Metal-Composite Gears. *Applied Composite Materials*, **26**, 817-833. https://doi.org/10.1007/s10443-018-9753-6

[5] He, Z., Zhou, D., Zhang, R., Ye, M., Lu, C., Liu, L., *et al*. (2025) Influence Mechanism of Beam Oscillation on Energy Density Distribution and Mechanical Properties of Steel/CFRP Joint by Direct Laser Welding. *Composite Structures*, **363**, Article 119133. https://doi.org/10.1016/j.compstruct.2025.119133

[6] Kazda, L. and Novotny, C. (2025) Effective Simplified Analytical and FEM Models for Load-Bearing Capacity of Unconventional Metal-Composite Shaft Joint. *Journal of Composite Materials*, **60**, 369-384. https://doi.org/10.1177/00219983251362312

[7] Yılmaz, T.G., Karadere, G. and Karpat, F. (2022) A Numerical Analysis of Hybrid Spur Gears with Asymmetric Teeth: Stress and Dynamic Behavior. *Machines*, **10**, Article 1056. https://doi.org/10.3390/machines10111056

[8] Herrmann, A.S., Zahlen, P.C. and Zuardy, I. (2005) Sandwich Structures Technology in Commercial Aviation. In: Thomsen, O., Bozhevolnaya, E. and Lyckegaard, A., Eds., *Sandwich Structures* 7: *Advancing with Sandwich Structures and Materials*, Springer-Verlag, 13-26. https://doi.org/10.1007/1-4020-3848-8_2

[9] Friedrich, H. and Schumann, S. (2001) Research for a "New Age of Magnesium" in the Automotive Industry. *Journal of Materials Processing Technology*, **117**, 276-281. https://doi.org/10.1016/s0924-0136(01)00780-4

[10] Mallick, P.K. (2010) Materials, Design and Manufacturing for Lightweight Vehicles. Woodhead Publishing.

[11] Sreedhar, S., Marla, D. and Guo, D. (2006) Fatigue Analysis for Axle Differential Cases. *SAE* 2006 *World Congress & Exhibition*, Detroit, 3-6 April 2006. https://doi.org/10.4271/2006-01-0779

[12] Kim, J. and Sham, M. (2000) Impact and Delamination Failure of Woven-Fabric Composites. *Composites Science and Technology*, **60**, 745-761. https://doi.org/10.1016/s0266-3538(99)00166-9

[13] Zweben, C. (2006) Thermal Materials Solve Power Electronics Challenges. *Power Electronics Technology*, **32**, 40-47. https://www.electronicdesign.com/technologies/eda/thermal-management/article/21188671/thermal-materials-solve-power-electronics-challenges

[14] Brockmann, W., Geiß, P.L., Klingen, J. and Schröder, B. (2009) Adhesive Bonding: Materials, Applications and Technology. Wiley-VCH. https://pdfs.semanticscholar.org/4e62/4751209d189e0b862db9600c7a5e736224ea.pdf

[15] Lindner, T., Saborowski, E., Scholze, M., Zillmann, B. and Lampke, T. (2018) Thermal Spray Coatings as an Adhesion Promoter in Metal/FRP Joints. *Metals*, **8**, Article 769. https://doi.org/10.3390/met8100769

[16] Mitschang, P., Velthuis, R., Emrich, S. and Kopnarski, M. (2009) Induction Heated Joining of Aluminum and Carbon Fiber Reinforced Nylon 66. *Journal of Thermoplastic Composite Materials*, **22**, 767-801. https://doi.org/10.1177/0892705709105969

[17] Changenet, C. and Velex, P. (2006) A Model for the Prediction of Churning Losses in Geared Transmissions—Preliminary Results. *Journal of Mechanical Design*, **129**, 128-133. https://doi.org/10.1115/1.2403727

[18] Witik, R.A., Payet, J., Michaud, V., Ludwig, C. and Månson, J.E. (2011) Assessing the Life Cycle Costs and Environmental Performance of Lightweight Materials in Automobile Applications. *Composites Part A*: *Applied Science and Manufacturing*, **42**, 1694-1709. https://doi.org/10.1016/j.compositesa.2011.07.024

[19] Das, S. (2011) Life Cycle Assessment of Carbon Fiber-Reinforced Polymer Composites. *The International Journal of Life Cycle Assessment*, **16**, 268-282. https://doi.org/10.1007/s11367-011-0264-z

[20] Elmarakbi, A. and Azoti, W. (2015) Novel Composite Materials for Automotive Applications: Concepts and Challenges for Energy-Efficient and Safe Vehicles. *International Journal of Smart and Nano Materials*, **6**, 90-100. https://sure.sunderland.ac.uk/id/eprint/5797/1/ICCST10-Paper_PL03.pdf

[21] Czerwinski, F. (2021) Current Trends in Automotive Lightweighting Strategies and Materials. *Materials*, **14**, Article 6631. https://doi.org/10.3390/ma14216631

[22] Mutasher, S.A. (2009) Prediction of the Torsional Strength of the Hybrid Aluminum/composite Drive Shaft. *Materials & Design*, **30**, 215-220. https://doi.org/10.1016/j.matdes.2008.05.024

[23] Ucsnik, S., Scheerer, M., Zaremba, S. and Pahr, D.H. (2010) Experimental Investigation of a Novel Hybrid Metal-Composite Joining Technology. *Composites Part A*: *Applied Science and Manufacturing*, **41**, 369-374. https://doi.org/10.1016/j.compositesa.2009.11.003

[24] Lambiase, F. and Paoletti, A. (2018) Friction-Assisted Clinching of Aluminum and CFRP Sheets. *Journal of Manufacturing Processes*, **31**, 812-822. https://doi.org/10.1016/j.jmapro.2018.01.014

[25] Page, M.J., McKenzie, J.E., Bossuyt, P.M., Boutron, I., Hoffmann, T.C., Mulrow, C.D., *et al.* (2021) The PRISMA 2020 Statement: An Updated Guideline for Reporting Systematic Reviews. *BMJ*, **372**, n71.

[26] Duflou, J.R., De Moor, J., Verpoest, I. and Dewulf, W. (2009) Environmental Impact Analysis of Composite Use in Car Manufacturing. *CIRP Annals*, **58**, 9-12. https://doi.org/10.1016/j.cirp.2009.03.077